NOTES AND CORRESPONDENCE

Setting the Length Scale in a Second-Order Closure Model of the Unstratified Bottom Boundary Layer[1]

H. O. MOFJELD AND J. W. LAVELLE

Pacific Marine Environmental Laboratory, Seattle, WA 98115

20 July 1983 and 20 December 1983

ABSTRACT

Frequently the mixing length l in second-order closure models is assumed to have a constant value $l_0 = \gamma L$ at large distances from the bottom with a magnitude proportional to the first moment L of turbulent intensity. Although it is often stated that turbulence closure model results are relatively insensitive to the value of mixing length parameter γ, we show that this is not the case for a second-order Level II model of the steady bottom boundary layer in an unstratified fluid. In particular, the eddy viscosity and diffusivity depend strongly on γ. Available oceanic data on geostrophic drag ratio lead to a value of γ of approximately 0.2–0.3. Atmospheric data for steady flow suggest a smaller value of 0.05–0.1 although the atmospheric observations are ambiguous about the choice of γ, possibly because it is difficult to find truly neutrally stratified and steady-state conditions in the bottom boundary layer. A value of γ between 0.18 and 0.20 is required for the model to match a similarity theory having a linear–exponential form for viscosity. Fitting an M_2 tidal current profile at a station in Admiralty Inlet, Washington, with an oscillatory analog of the model yields $\gamma = 0.20 \pm 0.04$.

1. Introduction

Closure models have proven useful in the study of geophysical fluids. One of the simplest of these models assumes that the turbulent intensity is determined by a local balance between shear generation and viscous dissipation. Called a Level II model by Mellor and Yamada (1974, 1982), this model produces simulations of unstratified boundary layers comparable to those of more sophisticated models.

For the present study, we use a Level II model with a form for the mixing length l proposed by Blackadar (1962):

$$l = \frac{\kappa z}{1 + \kappa z/l_0}, \tag{1}$$

that works well for models of unstratified boundary layers according to Weatherly and Martin (1978), Mellor and Yamada (1982) and Richards (1982). Near the bottom, the mixing length is the product of the von Kármán constant κ (=0.4 in this paper) and the height z as required for the classic logarithmic profile of velocity. For sufficiently large height, the mixing length approaches its asymptotic value l_0.

Following Weatherly and Martin (1978), Mellor and Yamada (1982), Du Vachat and Musson-Genon (1982) and Richards (1982), we assume that the asymptotic mixing length l_0 is determined by the vertical distribution of the turbulence

$$l_0 \equiv \gamma L = \gamma \frac{\int_{z_0}^{\infty} zq\,dz}{\int_{z_0}^{\infty} q\,dz}, \tag{2}$$

where L is the scale height of the turbulent intensity, z_0 the roughness length, q the turbulent intensity (square root of the turbulent kinetic energy) and γ is the mixing length parameter.

For oceanic conditions Weatherly and Martin (1978), Adams and Weatherly (1981) and Richards (1982) choose a value $\gamma = 0.3$. Mellor and Yamada (1974) recommend $\gamma = 0.1$ and Du Vachat and Musson-Genon (1982) a value $\gamma = 0.05$ based on the atmospheric data. We shall see that the size of γ affects many properties of the boundary layer including its vertical extent, viscosity, diffusivity, drag coefficient and veering angle. It is therefore important to have an accurate estimate of the mixing length parameter γ.

The steady mean velocity components U, V satisfy the equations

$$-fV = \frac{\partial}{\partial z}\left[A\frac{\partial U}{\partial z}\right], f(U - U_0) = \frac{\partial}{\partial z}\left[A\frac{\partial V}{\partial z}\right], \tag{3}$$

and the boundary conditions

$$U, V = 0 \quad \text{at} \quad z = z_0,$$
$$U, V \to U_0, 0 \quad \text{as} \quad z \to \infty. \tag{4}$$

The eddy viscosity A is written as the product

$$A = S_M q l, \tag{5}$$

[1] Contribution No. 651 of the NOAA/ERL Pacific Marine Environmental Laboratory.

where $S_M = c^{-1/3}$ (see Appendix) and c is the dissipation constant in the turbulent energy equation.

Writing the Reynolds stresses as products of the eddy viscosity and shear components, the balance between local generation of turbulence and dissipation is assumed to be given by

$$0 = -\left[-A\frac{\partial U}{\partial z}\right]\frac{\partial U}{\partial z} - \left[-A\frac{\partial V}{\partial z}\right]\frac{\partial V}{\partial z} - \frac{q^3}{cl}. \quad (6)$$

Richards (1982) among others has found that the principal balance in the full turbulent energy equation is due to these terms.

As Du Vachat and Musson-Genon (1982) point out, it is possible to write A in terms of the mixing length l and the shear alone:

$$A = l^2\left[\left(\frac{\partial U}{\partial z}\right)^2 + \left(\frac{\partial V}{\partial z}\right)^2\right]^{1/2}, \quad (7)$$

which is derived explicitly in the Appendix. This form (7) of A was used by Ekman (1905) with constant l.

Independence of l, U and V from the dissipation constant c (see Appendix) requires that the solution to the boundary value problem for mean velocity be subject to Rossby similarity as described by a number of authors including Rossby (1932), Rossby and Montgomery (1935), Csanady (1967), Blackadar and Tennekes (1968), Deardoff (1969), Wimbush and Munk (1970), Bowden (1978), Du Vachat and Musson-Genon (1982) and Brown (1982). Similarity theory allows the results of the numerical computations to be organized into a few relationships involving γ and the similarity scales. These scales are: the similarity height u_*/f, the similarity viscosity scale u_*^2/f and the surface Rossby number u_*/fz_0. The turbulent intensity q retains a weak $c^{1/3}$ dependence on the dissipation constant c (see Appendix). We solve the boundary value problem iteratively with standard numerical techniques (see Appendix).

2. Results

a. *Examples of profiles*

As shown in Fig. 1, the mean flow has a modest dependence on the mixing length parameter γ. For γ = 0.1, the velocity reaches its asymptotic value closer to the bottom than it does for γ = 0.2 and 0.3 and the maximum veering angle ϕ is greater for γ = 0.1. Over the range γ = 0.1–0.3, the turbulent intensity q and mixing length l (Fig. 2) change greatly. The most striking feature in the profiles of q is the increase in the vertical extent of the turbulence with increasing γ. The turbulence extends (Figs. 1 and 2) well above the region of strong shear near the bottom. The maximum turbulent intensity q_0 at the bottom ($z = z_0$) changes comparatively little over these values of γ because it is proportional to the friction velocity u_* which is relatively insensitive to γ (Table 1).

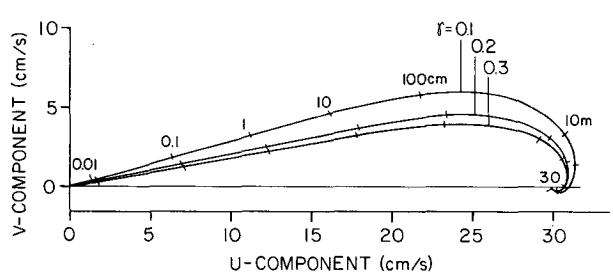

FIG. 1. Examples of Ekman spirals for the steady bottom Ekman layer in an unstratified ocean. The results were obtained by numerically integrating the second-order closure model for three values of the mixing length parameter γ = 0.1, 0.2 and 0.3. Representative heights above the bottom z_0 are marked on the Ekman spirals.

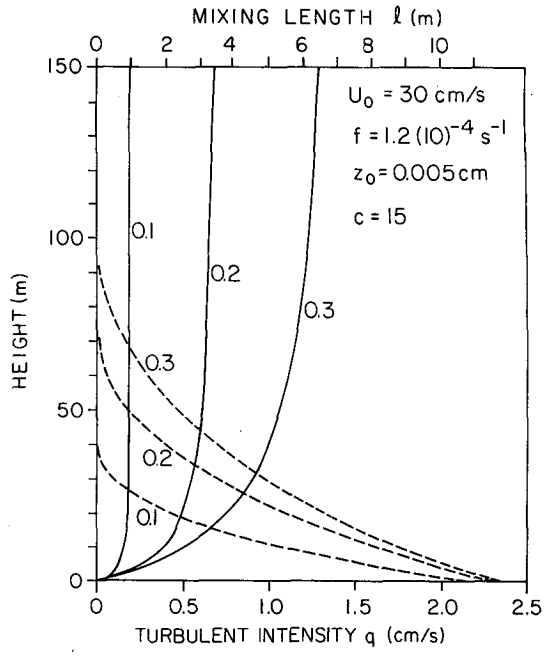

FIG. 2. Vertical profiles of mixing length l and turbulent intensity q corresponding to the three examples of Ekman velocity profiles shown in Fig. 1 for γ = 0.1, 0.2 and 0.3.

The sensitivity of the mixing length l (1) to γ depends on the height z above the bottom. Very near the bottom ($z < 1$ m), the mixing length $l \approx \kappa z$ is essentially independent of γ. Immediately above (Fig. 2), the profile of l for γ = 0.1 diverges from the other two profiles and makes a rapid transition to its asymptotic value. For the examples shown in Fig. 2, the γ = 0.2 profile diverges from that for γ = 0.3 at approximately z = 5 to 10 m. Well above the bottom ($z > 20$ m), there are major differences between the mixing lengths for the three values of γ.

Because the profiles of turbulent intensity q and mixing length l depend so strongly on the mixing length parameter γ, it is not surprising that the eddy viscosity A (5) increases rapidly (Fig. 3) with increasing γ in both amplitude and vertical extent. Each viscosity profile has the same general shape, increasing upward from a very small value ku_*z_0 at the bottom in response to the growth of the mixing length. The decrease in tur-

TABLE 1. Steady Ekman layer—summary of results for $U_0/fz_0 = 5.00 \times 10^7$

Mixing length parameter		γ = 0.1	γ = 0.2	γ = 0.3
Friction velocity	u_* (cm s^{-1})	0.875	0.934	0.949
Similarity height	u_*/f (m)	72.9	77.8	79.1
Surface Rossby number	u_*/fz_0	1.46×10^6	1.56×10^6	1.58×10^6
Geostrophic drag ratio	u_*/U_0	0.0292	0.0311	0.0316
Maximum veering angle	ϕ (deg)	16.4	12.0	10.4
Maximum turbulent intensity	q_0 (cm s^{-1})	2.16	2.30	2.34
Asymptotic mixing length	l_0 (m)	0.95	3.54	7.09
Height of maximum viscosity	z_{max} (m)	5.0	11.9	18.1
Maximum viscosity	A_{max} (cm^2 s^{-1})	41.6	125.2	206.4
Height where A = 5% A_{max}	$z_{5\%}$ (m)	33	63	88

bulent intensity q with height overwhelms the increase in l to form a maximum in viscosity (Fig. 3). Above the maximum the decrease in viscosity is controlled by the decrease in q. From the summary of results (Table 1) for the examples, we see that there is a fivefold increase in the maximum viscosity A_{max} and a 3.6-fold increase in its height z_{max} over the range γ = 0.1–0.3.

b. *Summary in similarity variables*

The results of numerical computations show that the height $z_{max} \approx 0.79\ \gamma u_*/f$ of maximum viscosity is very close to a linear function of γ. The maximum viscosity A_{max} satisfies a power law in γ of the form $A_{max} \approx 0.14\ \gamma^{1.3} u_*^2/f$. The asymptotic mixing length l_0 is nearly equal to a simple expression

$$l_0 \approx \gamma^2 u_*/f, \tag{8}$$

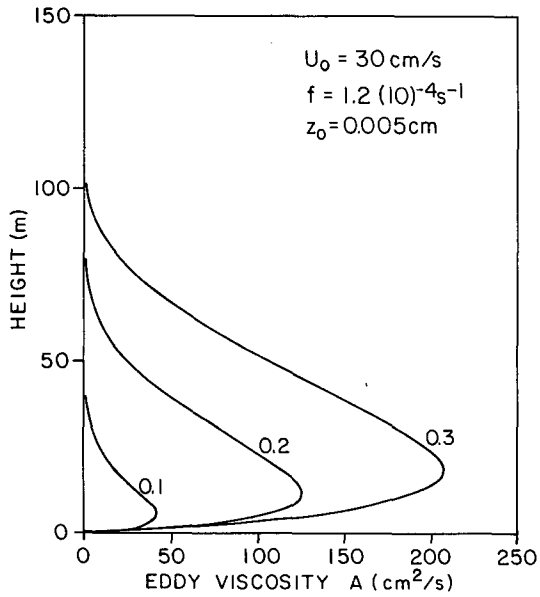

FIG. 3. As in Fig. 2 but of eddy viscosity A. Note the large increase in A with increasing γ.

from which it follows that

$$L \approx \gamma u_*/f. \tag{9}$$

Hence, γ gives the scale height L of the turbulence relative to the similarity height u_*/f.

Turning to the geostrophic drag ratio u_*/U_0 (Fig. 4), which is the ratio of bottom friction velocity u_* to the geostrophic velocity U_0, there is a decrease in the ratio as the surface Rossby number u_*/fz_0 increases. For a given value of u_*/fz_0, the ratio u_*/U_0 increases as γ is increased, although the ratio is less sensitive to changes in γ when γ is large (>0.2). There is an analogous behavior (Fig. 4) in the maximum veering angle ϕ between the flow just above the bottom and the

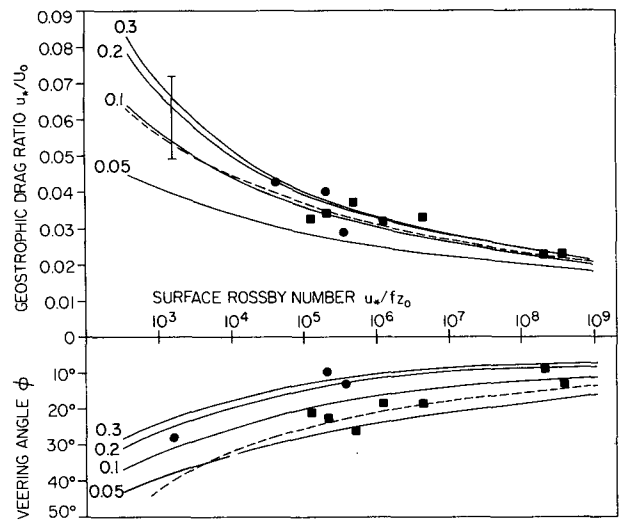

FIG. 4. Geostrophic drag ratio u_*/U_0 and maximum veering angle ϕ as functions of surface Rossby numbers u_*/fz_0 for different values of the mixing length parameter γ = 0.05, 0.1, 0.2 and 0.3. The dots are observed values from oceanic data as described by Lavelle and Mofjeld (1983) to which is added the data of Nakata (1981) and the squares are representative values from atmospheric data as reported by Csanady (1967). The dashed curves are from the empirical formulas [Eqs. (10) and (11)] with values A = 1.7 and B = 4.7 found by Blackadar (1962) from atmospheric data.

TABLE 2. Values of the constants A and B in the formulas for the ratio u_*/U_0 (10) and maximum veering angle ϕ (11) that are consistent with the Level II model at the value of surface Rossby number $u_*/fz_0 = 10^6$.

γ	u_*/U_0	ϕ	A	B
0.05	0.0252	23.9°	−0.70	6.43
0.10	0.0298	16.8°	0.97	3.88
0.20	0.0326	12.2°	1.82	2.59
0.30	0.0334	10.5°	2.04	2.18

geostrophic flow U_0 above the Ekman layer. The few estimates of u_*/U_0 and ϕ that are available from the oceanic literature (see Lavelle and Mofjeld, 1983, for a detailed description and references for the oceanic estimates as well as Nakata, 1981; the atmospheric observations are from Csanady, 1967) show the general decrease of both quantities with surface Rossby number u_*/fz_0.

There may be a systematic difference between observed veering angles from atmospheric and oceanic data. The atmospheric angles favor a small value of $\gamma < 0.1$ while the oceanic angles favor a larger value of γ. One reason for the scatter in observed atmospheric values may be that the atmosphere does not remain unstratified long enough to develop a steady profile and is still under the influence of earlier stratification (J. A. Businger and J. E. Overland, private communication, 1983). Other reasons for the scatter in both the atmospheric and oceanic observations include secondary rolls (Brown, 1980), sloping bottoms (Weatherly, 1975; Weatherly and Martin, 1978) and the influence of tidal motions (Weatherly, 1975).

3. Selection of a value for γ

a. Comparison with Rossby-number similarity theory

It is useful to compare the results of the Level II model with those of other formulations of the bottom Ekman layer. The Rossby-number similarity theory as described, e.g., by Brown (1982) matches a logarithmic layer near the bottom to an exterior Ekman layer in which the eddy viscosity is a constant. Formulas are then obtained for the geostrophic drag coefficient u_*/U_0 and the maximum veering angle ϕ such that

$$\frac{u_*}{U_0} = \kappa \left\{ B^2 + \left[\ln\left(\frac{u_*}{fz_0}\right) - A \right]^2 \right\}^{-1/2}, \tag{10}$$

$$\phi = \arcsin\left[B \left(\frac{u_*}{U_0}\right) \kappa^{-1} \right], \tag{11}$$

where the similarity functions A (not to be confused with the eddy viscosity) and B are fit to observations. These formulas can also be derived from asymptotic theory without specifying the detailed form of the viscosity well above the bottom (i.e., Blackadar and Tennekes, 1968).

We require that u_*/U_0 and ϕ from Eqs. (10) and (11) be equal to the corresponding quantities from the Level II model for the same surface Rossby number u_*/fz_0. The constants A and B then become functions of γ as shown in Table 2. Values of $A = 1.7$ and $B = 4.7$ obtained from atmospheric observations (Blackadar, 1962) tend to favor a small value of γ although no value gives simultaneously values of u_*/U_0 and Φ corresponding to this pair of A and B values. Based on more recent atmospheric observations, Du Vachat and Musson-Genon (1982) prefer a value of $\gamma = 0.05$ with some reservations about the agreement between the theory and observations. There is sufficient scatter in the observations of A and B as presented by Brown (1982) that any value of γ between 0.05 and 0.3 gives values of A and B within this scatter. One may conclude that the corresponding quantities A and B from the Level II model are insensitive to the value of γ within present experimental error.

Another treatment of the bottom Ekman layer is based on the similarity theory (Arya, 1973; Businger and Arya, 1974) in which the eddy viscosity is given a form

$$A' = \kappa u_* z e^{-z/z'_{\max}}, \tag{12}$$

where the height of maximum viscosity is

$$z'_{\max} = u_*^2 (fU_0 \sin\phi)^{-1}. \tag{13}$$

This form of viscosity has a shape similar to those shown in Fig. 3. We can obtain a value for γ by requiring that the height $z_{\max}$ from the Level II model be equal to the form (13) where the values of u_*/U_0 and ϕ are taken from Fig. 4. Table 3 shows that this value is $\gamma = 0.20$ and that it is independent of surface Rossby number u_*/fz_0. Matching the maximum values of viscosity $A_{\max}$ gives a similar result $\gamma = 0.18$.

b. An estimate from observed tidal currents

The steady Ekman layer is directly analogous to the bottom boundary layer associated with unidirectional, oscillatory flow. The frequency of oscillation replaces the Coriolis parameter and the out-of-phase velocity

TABLE 3. Comparison of the height of maximum viscosity $z_{\max}$ for the Level II model with that from the similarity theory ST of Businger and Arya (1974). The heights have been divided by the similarity scale u_*/f. Note the excellent agreement for $\gamma = 0.20$. Matching the value of the maximum viscosity gives $\gamma = 0.18$.

	$u_*/fz_0 =$							
	10^4		10^5		10^6		10^7	
γ	II	ST	II	ST	II	ST	II	ST
0.10	0.069	0.103	0.069	0.103	0.069	0.103	0.069	0.103
0.20	0.153	0.150	0.153	0.153	0.153	0.154	0.153	0.152
0.30	0.236	0.171	0.236	0.179	0.236	0.183	0.236	0.182

component replaces the steady component perpendicular to the geostrophic flow. For the purpose of estimating γ, we shall consider the M_2 tidal current profile observed at Station MESA 10 (48°1.8'N, 122°37.8'W) in Admiralty Inlet, Washington, which is a long, narrow inlet leading to Puget Sound (see Cannon *et al.*, 1979, for a description of the observations). We shall neglect the effect of time-dependence and other tidal constituents in the eddy viscosity on the current profile (the effects of time-dependent viscosity are discussed by Lavelle and Mofjeld, 1983). The least-square fit (Fig. 5) of the Level II model to the M_2 current amplitude profile gives a value for the mixing length parameter $\gamma = 0.20 \pm 0.04$ that is consistent with that obtained using the similarity theory of Businger and Arya (1974).

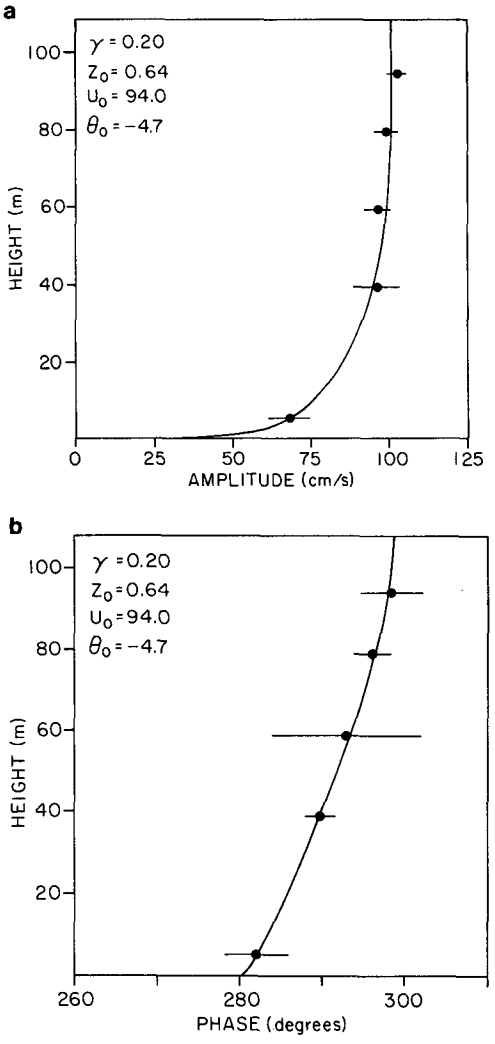

FIG. 5. (a) M_2 tidal amplitudes and (b) Greenwich phases for the principal axis (171° True) at Station MESA 10 (48°1.8'N, 122°37.8'W) in Admiralty Inlet, Washington. The estimates (dots) of observed amplitude and phase at five heights were obtained via response tidal analyses. The crossbars through the data points are 99% confidence limits based on six 9-day analyses. The curves are least square fits of an oscillatory Level II model to the observations using the four parameters γ, z_0, U_0 and a phase shift θ_0 independent of height.

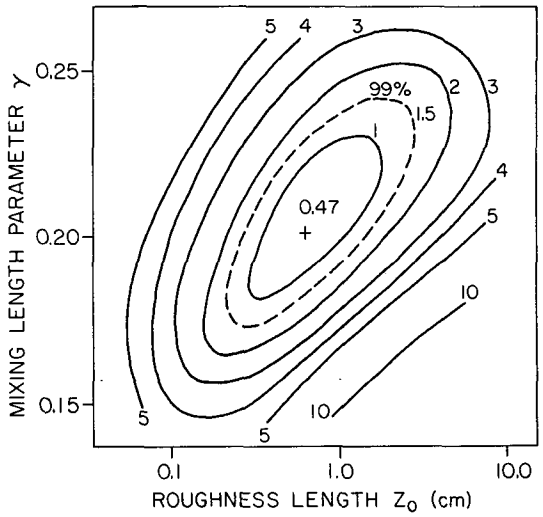

FIG. 6. Confidence surface (contours of summed square deviations in units of 100 $cm^2\ s^{-2}$) for the fit (Fig. 5) of the oscillatory Level II model to observed M_2 tidal currents at Station MESA 10 in Admiralty Inlet, Washington. The surface was obtained by contouring the optimal square deviations for a range of γ and z_0. The dashed contour is the 99% confidence limit.

The 99% confidence limits on γ were obtained from the confidence surface (Fig. 6). The inclination of the contours relative to the γ and z_0 axes shows that simultaneous adjustments of the two parameters can produce nearly as good a fit to the observations as the best values. The optimal value of z_0 is relatively large (0.64 cm) and corresponds to roughness elements on the bottom of order $\sim 30 \times 0.64 = 19$ cm. This is reasonable for Admiralty Inlet which is known to have a rough, rocky bottom.

4. Conclusions

In this paper, we have considered how one empirical constant γ affects the results of a Level II model for the bottom Ekman layer. Because of Rossby similarity inherent in the model, all the vertical length scales in the solution are proportional to the similarity height u_*/f. The speed profile and bottom stress are not very sensitive to the mixing length parameter γ. Its effect on the veering angle is greater. Perhaps the most important role that γ plays in the model is to fix the vertical scale of the turbulence and hence, the magnitude and distribution of the eddy viscosity. There is some ambiguity concerning the value of γ obtained from oceanic and atmospheric data. The available but sparse oceanic data on the geostrophic drag ratio for the steady Ekman layer suggest $\gamma \approx 0.2$–0.3. Such large values imply relatively large values for the eddy viscosity.

Requiring that the Level II model match the similarity theory of Businger and Arya (1974), fixes the value of the mixing length parameter $\gamma = 0.18$–0.20. This range for γ is consistent with that ($\gamma = 0.20 \pm 0.04$) obtained by fitting the oscillatory analog of the Level II model to M_2 tidal currents at a station in Admiralty Inlet, Washington.

Acknowledgments. The authors wish to thank J. E. Overland and J. A. Businger for many helpful discussions of the Ekman layer and the relative advantages of the second-order closure and similarity approaches to the study of boundary layers. The authors also wish to thank the anonymous reviewers for their helpful comments. This work was supported in part by the Office of Marine Pollution Assessment under the LRERP/Section 202 Program and by the Environmental Research Laboratories, National Oceanic and Atmospheric Administration. The work was also supported in part by the Minerals Management Service through interagency agreement with the National Oceanic and Atmospheric Administration under which a multiyear program responding to needs of petroleum development of the Alaska continental shelf is managed by the Outer Continental Shelf Environmental Assessment Program Office.

APPENDIX

1. Derivation of the form (7) for the viscosity

Substituting the form (5) for the eddy viscosity into (6) and solving for the turbulent intensity gives

$$q = (cS_M)^{1/2} l \left[\left(\frac{\partial U}{\partial z} \right)^2 + \left(\frac{\partial V}{\partial z} \right)^2 \right]^{1/2} \tag{A1}$$

from which we obtain an expression for the eddy viscosity in terms of the mixing length and shear

$$A = (cS_M^3)^{1/2} l^2 \left[\left(\frac{\partial U}{\partial z} \right)^2 + \left(\frac{\partial V}{\partial z} \right)^2 \right]^{1/2}. \tag{A2}$$

Since the turbulence production represented by the first two terms of the turbulent energy equation (6) cannot depend on how the turbulence is dissipated (independent of c), the last term of (6) must also be independent of c. Since c is a constant while l (1) is a function of z (and perhaps c), q must be proportional to $c^{1/3}$. Because l, $\partial U/\partial z$ and $\partial V/\partial z$ are functions of z, S_M is a constant and q is proportional to $c^{1/3}$, Eq. (A1) requires that

$$(cS_M)^{1/2} = c^{1/3}, \tag{A3}$$

or the parameter S_M is

$$S_M = c^{-1/3}. \tag{A4}$$

Therefore, by Eq. (A2) the eddy viscosity is

$$A = l^2 \left[\left(\frac{\partial U}{\partial z} \right)^2 + \left(\frac{\partial V}{\partial z} \right)^2 \right]^{1/2}, \tag{A5}$$

and the turbulent intensity becomes

$$q = c^{1/3} l \left[\left(\frac{\partial U}{\partial z} \right)^2 + \left(\frac{\partial V}{\partial z} \right)^2 \right]^{1/2}. \tag{A6}$$

The mixing length l and velocity U, V might still be implicit functions of c. However, when (A6) is inserted into expression (2) for the asymptotic mixing length l_0, the mixing length l (1) looses any explicit dependence on c. Since Eqs. (1), (2), (3), (4) and (7) in the text form a closed set without explicit dependence on c, they do not have any implicit dependence either. That is, l and U and V are independent of c and thus, of the Reynolds number.

2. Numerical method

The solutions for the steady Ekman problem were obtained by integrating the complex velocity equation formed from (3) using a fourth-order Runge-Kutta scheme. The velocity equation was integrated downward from the surface and then renormalized to match the boundary condition at the bottom. The vertical spacing of the grid was decreased near the bottom to allow for the large shear there. The values of z at each odd grid index s was found by solving the implicit formula

$$s = az + b \log(z) + c. \tag{A7}$$

The constants a, b, c, were chosen so that half of the grid points lay below a height of 1 m. The even grid points were halfway between the odd ones to satisfy requirements of the Runge-Kutta scheme. A total of 2001 grid points were used.

All variables were in cgs units. The geostrophic velocity ($U_0 = 30$ cm s^{-1}) and Coriolis parameter ($f = 1.2 \times 10^{-4}$ s^{-1}) were fixed. The range of surface Rossby number was scanned by changing the roughness length z_0 from 0.5 m to 0.0005 cm. The depth was taken to be 150 m except at the Admiralty Inlet Station (108 m); free-slip (zero shear) was assumed as the surface boundary condition. Fixing U_0 and f and varying z_0 is equivalent to varying the external Rossby number U_0/fz_0. It produces a relatively constant ratio of the similarity height u_*/f to the total depth, which is numerically convenient. To prevent numerical problems, a small viscosity was added to that given by second-order closure. This small addition increased linearly from zero at $z = z_0$ to ~ 1 cm^2 s^{-1} at the surface.

Using a initial profile of viscosity based on the linear–exponential form, the first profiles of the dynamic variables were obtained. Thereafter, the Level II viscosity (5) was used. The calculations were repeated using the

previous estimates of viscosity until the friction velocity u_* was stable within 1×10^{-3} cm s^{-1}. Instabilities in the iteration scheme were avoided by setting the eddy viscosity equal to the mean of the previous two profiles.

REFERENCES

Adams, C. E., and G. L. Weatherly, 1981: Some effects of suspended sediment stratification on an oceanic boundary layer. *J. Geophys. Res.*, **86,** 4161–4172.

Arya, S. P. S., 1973: Neutral planetary boundary layer above a non-homogeneous surface. *Geophys. Fluid Dyn.*, **4,** 333–355.

Blackadar, A. K., 1962: The vertical distribution of wind and turbulent exchange in a neutral atmosphere. *J. Geophys. Res.*, **67,** 3095–3120.

——, and H. Tennekes, 1968: Asymptotic similarity in neutral barotropic planetary boundary layers. *J. Atmos. Sci.*, **25,** 1015–1020.

Bowden, K. F., 1978: Physical problems of the benthic boundary layer. *Geophys. Surveys,* **3,** 255–296.

Brown, R. A., 1980: Longitudinal instabilities and secondary flows in the planetary boundary layer: a review. *Rev. Geophys. Space Phys.*, **18,** 683–697.

——, 1982: On two-layer models and the similarity functions for the PBL. *Bound.-Layer Meteor.*, **24,** 451–463.

Businger, J. A., and S. P. S. Arya, 1974: Height of the mixed layer in the stably stratified planetary boundary layer. *Advances in Geophysics,* Vol. 18A, Academic Press, 73–92.

Cannon, G. A., N. P. Laird and T. L. Keefer, 1979: Puget Sound circulation. Final rep. for FY-77-78. NOAA Tech. Memo. ERL MESA-40, 55 pp.

Csanady, G. T., 1967: On the "resistance law" of a turbulent Ekman layer. *J. Atmos. Sci.*, **24,** 467–471.

Deardoff, J. W., 1969: Similarity principles for numerical integrations of neutral barotropic planetary boundary layers and channel flows. *J. Atmos. Sci.*, **26,** 763–767.

Du Vachat, R., and L. Musson-Genon, 1982: Rossby similarity and turbulent formulation. *Bound.-Layer Meteor.*, **23,** 47–68.

Ekman, V. W., 1905: On the influence of the earth's rotation on ocean-currents. *Ark. Mat. Astron. Fys.*, **2,** 52 pp.

Lavelle, J. W., and H. O. Mofjeld, 1983: Effects of time-dependent viscosity on oscillatory turbulent channel flow. *J. Geophys. Res.*, **12,** 7607–7616.

Mellor, G. L., and T. Yamada, 1974: A hierarchy of turbulence closure models for planetary boundary layers. *J. Atmos. Sci.*, **31,** 1791–1806. (Corridgendum, 1977. *J. Atmos. Sci.*, **34,** 1482)

——, and ——, 1982: Development of a turbulence closure model for geophysical fluid problems. *Rev. Geophys. Space Phys.*, **20,** 851–875.

Nakata, K., 1981: Observations of the bottom boundary layer on the continental shelf. *J. Oceanogr. Soc. Japan,* **37,** 94–99.

Richards, K. J., 1982: Modeling the benthic boundary layer. *J. Phys. Oceanogr.*, **12,** 428–439.

Rossby, C. G., 1932: A generalization of the theory of the mixing length with application to atmospheric and oceanic turbulence. *Met. Pap.*, M.I.T., **1,** 36 pp.

——, and R. B. Montgomery, 1935: The layer of frictional influence in wind and ocean currents. *Pap. Phys. Oceanogr. Meteor.*, **3,** 101 pp.

Weatherly, G. L., 1975: A numerical study of time-dependent turbulent Ekman layers over horizontal and sloping bottoms. *J. Phys. Oceanogr.*, **5,** 288–299.

——, and P. J. Martin, 1978: On the structure and dynamics of the oceanic bottom boundary layer. *J. Phys. Oceanogr.*, **8,** 557–570.

Wimbush, M., and W. Munk, 1970: The benthic boundary layer. *The Sea,* Vol. 4, Part 1, A. E. Maxwell, Ed., Wiley-Interscience, 730–758.